

## Supplementary material

### SIMULATION OF EXPERIMENTAL CONFIGURATIONS

The method adopted to simulate and compute the neutrino interaction spectra for is described for both the Hyper-K and ESS $\nu$ SB experimental configurations.

**Hyper-K simulation:** An experiment corresponding to ten years of data taking with a 187 kt of water target and an antineutrino beam mode exposure three times larger than the neutrino one, as reported in [1], is simulated with the NEUT neutrino event generator using the SF CCQE cross-section model and the T2K/Hyper-K flux [2, 3]. The Prob3++ software was used to calculate the neutrino oscillation probabilities [4] and, for a given set of oscillation parameter values, the number of expected events was computed as:

$$N_{osc}(E_\nu) = \sum_{E_\nu} \Phi(E_\nu) \times \sigma(E_\nu) \times N_{tgt} \times N_{POT} \times P_{osc}(E_\nu) \quad (1)$$

where  $E_\nu$  is the neutrino energy,  $\Phi$  is the incoming neutrino flux (before oscillations occur),  $\sigma$  is the interaction cross section,  $N_{tgt}$  is the number of target nuclei,  $N_{POT}$  is the number of accelerator protons on target (POT) and  $P_{osc}$  is the oscillation appearance probability, either  $\nu_\mu \rightarrow \nu_e$  for electron neutrino events or  $\bar{\nu}_\mu \rightarrow \bar{\nu}_e$  for electron antineutrino events. Since  $N_{osc}$  corresponds to the expected number of CCQE events without considering detector efficiencies, smearing effects or background, the resulting total number of events is slightly different from the numbers reported in [1].

**ESS $\nu$ SB simulation:** A method analogous to the one adopted for the Hyper-K simulation was used but using the neutrino and antineutrino flux distributions of the ESS $\nu$ SB concept experiment. The fiducial active mass was taken to be 200 kt. The same run plan as for Hyper-K was assumed (three times more antineutrino beam than neutrino beam). The flux at a baseline of 100 km was obtained from the ESS $\nu$ SB CDR [5] using a plot-digitizer [6]. It is then additionally scaled to a FD baseline of 360 km, assuming a radial broadening ( $\sim 1/r^2$ ) of the beam. The neutrino and antineutrino oscillated CCQE event distributions predicted by the NEUT SF model are shown in fig. 1, using the same nominal oscillation parameters as used throughout the article and a baseline of 360 km.

The peak is at a lower energy and spans a wider range of angles with respect to the Hyper-K case, especially for antineutrinos. Given that there are more events in the region of kinematic phase space shown, in fig. 2 of the main article, to be susceptible to variations of  $R_{\nu_e/\nu_\mu}$ ,

it is unsurprising that a larger uncertainty is found for ESS $\nu$ SB compared to the Hyper-K experiment.

### STATISTICAL UNCERTAINTIES

The SF and LFG model predictions were extracted using a NEUT Monte-Carlo simulation and are thus subject to a statistical uncertainty related to the number of events generated. For this analysis, 300 million events were produced per neutrino flavour and model. However, even with large numbers of events, the statistical uncertainty on cross-section ratios (or double ratios) is important to consider. The relative statistical uncertainty on a cross-section ratio can be calculated as:

$$\delta(E_\nu, \theta) / (N_A/N_B) = \sqrt{1/N_A(E_\nu, \theta) + 1/N_B(E_\nu, \theta)}, \quad (2)$$

where  $N_A$  and  $N_B$  are the number of events within some bin of  $E_\nu$ ,  $\theta$  of one of the flavours. Fig. 2 shows the relative statistical uncertainty on the cross-section ratios considered within this article, using the two dimensional binning shown in the majority of figures (10 degree bins in  $\theta$  and 100 MeV bins in  $E_\nu$ ). Whilst the statistical uncertainty within individual bins shown can be up to  $\sim 10\%$ , it is usually at the  $\sim 0-3\%$  level in the regions of interest for this article.

When double ratios (RR) are considered (i.e. in the ratio of model predictions of two cross section ratios) the statistical uncertainty enters four times when comparing two NEUT-generated models (note that the calculations from the hadron tensor tables are analytical and have no statistical uncertainty). The size of the relative uncertainty on the double ratios of NEUT cross sections are also shown in fig. 2, reaching  $\sim 20\%$  for some bins at very high energies and angles but is generally less than  $\sim 5\%$  in regions of interest for this article.

Overall, it must be noted that the relative statistical uncertainty on the systematic uncertainties calculated within this article, which considers the entire integrated phase space, will be much smaller than the uncertainty on individual bins.

### INVESTIGATING THE SOURCE OF THE NUCLEAR MODEL UNCERTAINTIES

The cause of differences in model predictions of  $\langle \bar{\nu}_e / \bar{\nu}_\mu \rangle$  or  $\nu_e / \bar{\nu}_e$  cross-section ratios has previously been assigned to a number of physical processes. The calculation of associated model-spread based uncertainty metrics ( $\Delta_{\nu_e/\nu_\mu}$ ,  $\Delta_{\bar{\nu}_e/\bar{\nu}_\mu}$ ,  $\Delta_{\nu_e/\bar{\nu}_e}$ ) for cross-section

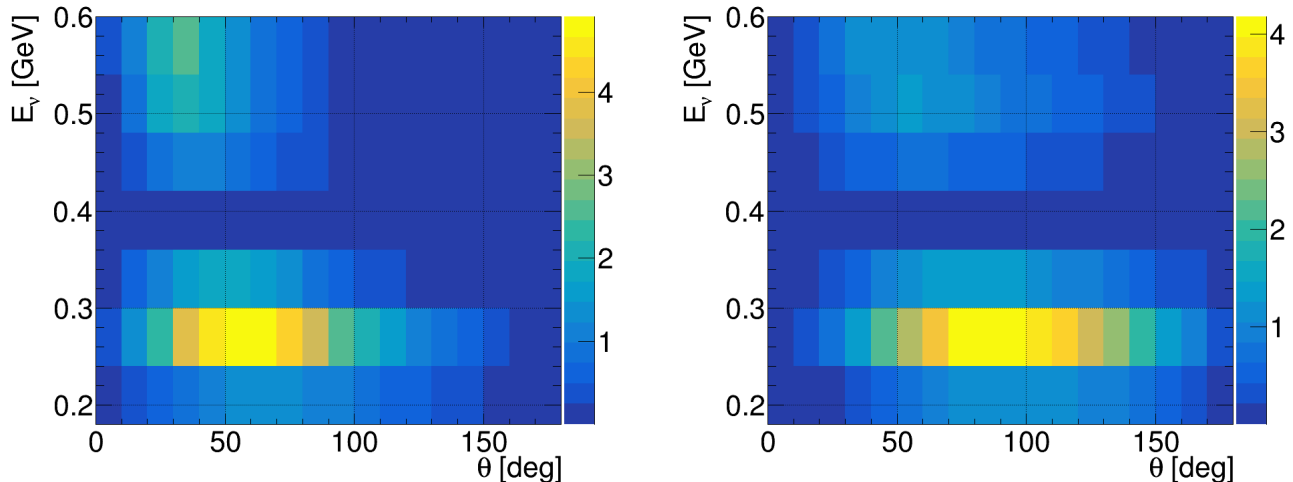


FIG. 1: The digitised ESS $\nu$ SB oscillated NEUT SF-based event rates for  $\nu_\mu$  (left) and  $\bar{\nu}_\mu$  (right) expected at the far detector. The X and Y axes show respectively the outgoing lepton angle and the neutrino energy. The Z-axis shows the relative proportion of the event rate in each bin as a percentage.

integrated over the T2K/Hyper-K flux is performed using sets of model that contain systematically different physics in an attempt to establish underlying sources of the uncertainty. The results are shown in fig. 3 of the main article, considering the full list of model shown in tab. I. This section contains a more detailed breakdown of the impact of each model variation.

**Influence of  $M_A^{QE}$ :** The nominal values of  $M_A^{QE}$  in the HF-CRPA and SF models are 1.03 and 1.21 GeV respectively. The impact of changing  $M_A^{QE}$  to 1.03 GeV in SF, broadly spanning the range of values implied by cross-section measurements [7], is investigated as a source of uncertainty. The uncertainty metrics used throughout the article are calculated between SF with the two different values of  $M_A^{QE}$ . The resulting uncertainties are negligible (less than 0.1%).

**Pauli blocking:** Pauli blocking introduces a region at small angles and low energies where, counter intuitively, the muon neutrino cross section becomes larger than the electron neutrino cross section, as discussed in [8, 9]. In order to investigate the influence of Pauli blocking the nominal SF model is compared to a version in which the Pauli blocking was disabled.

A comparison of the cross section predicted by NEUT's SF model with and without Pauli blocking is shown in fig. 3. It is clear that the only region of the phase space affected by Pauli blocking is at low neutrino energies and forward lepton angle, where the  $\nu_\mu$  ( $\bar{\nu}_\mu$ ) cross section becomes lower than the  $\nu_e$  ( $\bar{\nu}_e$ ) one. This region is also affected by a relatively large deviation from unity in  $RR_{\nu_e/\nu_\mu}^{\text{SF}/(\text{SF w/o PB})}$ . However, this is also a region of very low cross section in all models and so barely overlaps

with the distribution of events expected at the Hyper-K or ESS $\nu$ SB FDs.

The resulting systematic uncertainties for all metrics considered due to turning Pauli blocking on and off in the SF model is at the level of 0.2% or less. This small impact is because Pauli blocking affects a very narrow region of kinematic phase space which contains only a very small portion of the total cross section.

**Inclusion of CRPA nucleon correlations:** The HF-CRPA model is based on a mean-field HF approach with CRPA corrections to model long-range nuclear correlations. The influence of these corrections on the derived uncertainties is calculated as in the previous paragraphs. Overall their inclusion leads to an uncertainty of less than 0.2% for all metrics.

**Final State Interactions:** A major difference between the HF-CRPA and SF models is the inclusion of FSI in the calculation of the inclusive cross section via the consideration of the distortion of the outgoing nucleon wavefunction. This was identified as part of the cause of the HF-CRPA forward scattering features shown in the main article and discussed in [8]. The impact of such FSI was studied within the HF-CRPA model by turning its effects on and off. The derived uncertainty was found to be less than 0.3%, for all metrics. This is due to the small overlap between the heavily impacted forward lepton region and the phase space covered by the electron (anti)neutrino appearance events expected at the Hyper-K (or T2K) FD.

**Nuclear model:** By far the largest differences in model predictions of  $\langle \bar{\nu} \rangle_e / \langle \bar{\nu} \rangle_\mu$  or  $\nu_e / \bar{\nu}_e$  cross-section

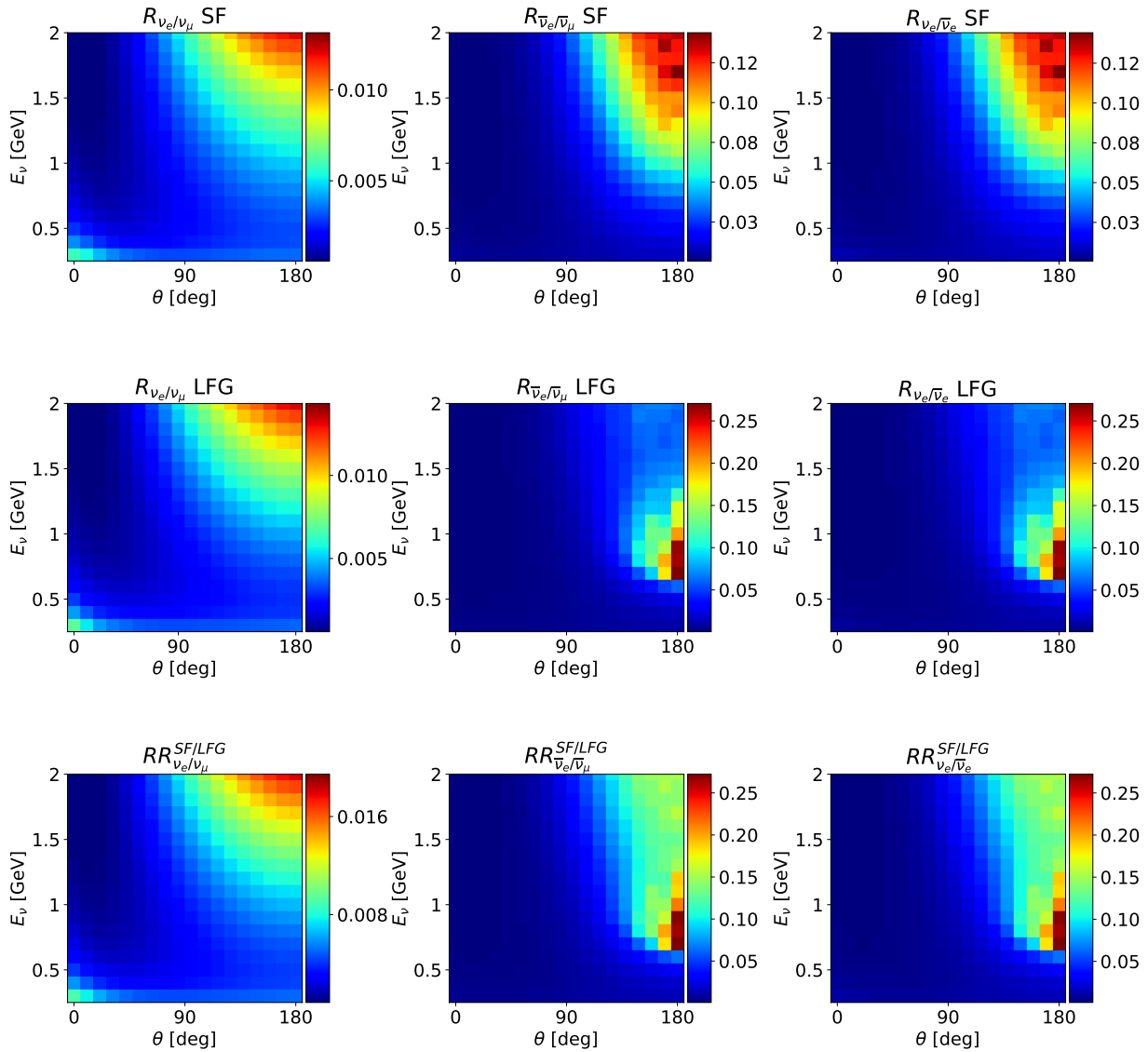


FIG. 2: The relative fractional statistical uncertainty on single and double cross-section ratios considered for the SF and LFG models.

ratios is found when comparing any HF-based or RMF-based model to any SF-based or LFG-based model. Given that the effect of changing any individual component of the models was found to be small, the difference in the ratios is likely driven by the treatment of the nuclear ground state. Whilst the difference in the cross-section ratios between models is dominated by the very forward and backward regions, the impact on Hyper-K oscillated  $\nu_e$  and  $\bar{\nu}_e$  event rates remains driven by the smaller differences at intermediate scattering angles.

### INVESTIGATING THE UNCERTAINTY RELATED TO DIFFERENCES BETWEEN CARBON AND OXYGEN NUCLEAR MODELS

It is interesting to consider the sensitivity of the model predictions of  $\langle \bar{\nu}_e \rangle / \langle \bar{\nu}_\mu \rangle$  or  $\nu_e / \bar{\nu}_e$  cross-section ratios to the target nucleus considered, particularly for the case of differences between oxygen and carbon target nuclei (as these are the predominant nuclear target in T2K/Hyper-K's near detector and far detector respectively). In order to evaluate this, the cross-section calculation from HF-CRPA on carbon nucleus was compared with cross-section calculations using an oxygen nucleus. The differences in the cross-section ratios on a carbon and oxygen target are found to be small compared to differences be-

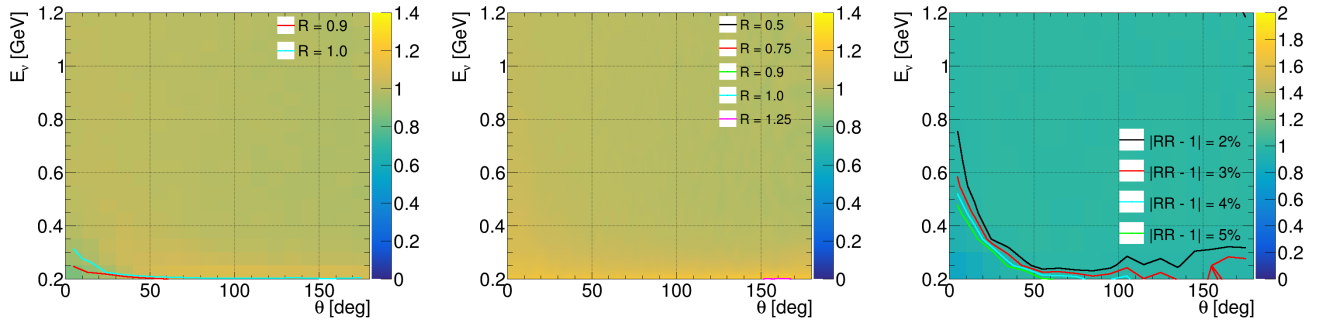


FIG. 3:  $R_{\nu_e/\nu_\mu}^{\text{SF}}$  (left),  $R_{\nu_e/\nu_\mu}^{\text{SF w/o PB}}$  (centre) and  $RR_{\nu_e/\nu_\mu}^{\text{SF / (SF w/o PB)}}$  (right) are shown. The double ratio of those two first plots is shown on the right. The contour lines highlight the regions where the single ratio significantly deviates from unity and are built using a bi-linear interpolation based on the four nearest bin centres [10]. Note that this uses unseen bins for neutrino energies less than 0.2 GeV.

tween models on a single target. This suggests that, at least for the HF-CRPA model considered, that carbon-to-oxygen differences appear to have a subdominant effect on the cross-section ratios of interest.

- 
- [1] K. Abe et al. (Hyper-Kamiokande), (2018), [arXiv:1805.04163](https://arxiv.org/abs/1805.04163) [physics.ins-det].
- [2] K. Abe et al. (T2K), *Phys. Rev. D* **87**, 012001 (2013), [Addendum: *Phys. Rev. D* **87**, no.1, 019902 (2013)], [arXiv:1211.0469](https://arxiv.org/abs/1211.0469) [hep-ex].
- [3] <http://t2k-experiment.org/wp-content/uploads/T2Kflux2016.tar>, accessed: 07/12/2022.

- [4] <https://github.com/rogerwendell/Prob3plusplus>, accessed: 07/12/2022.
- [5] A. Alekou et al., (2022), [10.1140/epjs/s11734-022-00664-w](https://arxiv.org/abs/2206.01208), [arXiv:2206.01208](https://arxiv.org/abs/2206.01208) [hep-ex].
- [6] A. Rohatgi, “Webplotdigitizer: Version 4.6,” (2022).
- [7] C. Wilkinson et al., *Phys. Rev. D* **93**, 072010 (2016), [arXiv:1601.05592](https://arxiv.org/abs/1601.05592) [hep-ex].
- [8] A. Nikolakopoulos, N. Jachowicz, N. Van Dessel, K. Niewczas, R. González-Jiménez, J. M. Udías, and V. Pandey, *Phys. Rev. Lett.* **123**, 052501 (2019), [arXiv:1901.08050](https://arxiv.org/abs/1901.08050) [nucl-th].
- [9] A. M. Ankowski, *Phys. Rev. C* **96**, 035501 (2017), [arXiv:1707.01014](https://arxiv.org/abs/1707.01014) [nucl-th].
- [10] F. Rademakers, R. Brun, P. Canal, et al., “ROOT - An Object-Oriented Data Analysis Framework. root-project/root: v6.10/04,” (2017).